JOURNAL OF MATERIALS SCIENCE **37** (2002) 4663–4668

Microstructure formation processes in melt spun and bulk undercooled Fe- and Ni-base alloys

V. V. MASLOV, V. K. NOSENKO
G. V. Kurdyumov Institute for Metal Physics of the National Ukrainian Academy of Sciences, 36 Vernadsky Av., UA-03680 Kiev-142, Ukraine
E-mail: maslov@imp.kiev.ua

M. JURISCH
Freiberger Compound Materials GmbH, Am Junger Lowe Schacht 5, D-09599 Freiberg, Federal Republic of Germany

Microstructures of dynamically undercooled (melt spun) Fe-base alloys characterized by a post-dendritic needle-like growth morphology were shown to be essentially identical to those of bulk undercooled samples with $\Delta T > 190$–200 K. Nonequilibrium crystallization is accompanied by the formation of internal stresses and defects which can lead to relaxation processes (polygonization, recrystallization) during the cooling procedure changing the asquenched microstructure. The mechanism and degree of these transformation processes are determined by the level of frozen-in microstresses, the cooling rate in the solid state, and the lattice structure of the alloys.

1. Introduction

A variety of microstructures, equiaxed and columnar grain, cellular, dendritic and post-dendritic, has been observed across rapidly quenched ribbons independent of the solidification method used. They are the result of either the actual local solidification process, post-solidification transformations, or both. The local solidification can be well described by thermal process models which include local differences (lift-off) and time dependence (shrinkage during wheel contact) of the heat transfer coefficient and thereby prescribe the field of local interface velocities and effective diffusion length in the solid state across the ribbon [1]. Solidification during rapid quenching of ribbons has been treated both as a growth into a undercooled melt (negative temperature gradient ahead of the interface) and of steady-state growth into a melt with a positive temperature gradient [2, 3]. To elucidate this question important for microstructural control during ribbon formation, comparisons were made of the microstructure and solidification behaviour of melt spun ribbons and bulk undercooled alloys. Until now, the reported results are contradictory. For example, it was concluded in [4] from an extensive study of the microstructure of chill block melt spun Ni-Mo-alloys underwell defined experimental conditions pertaining to wheel speed and alloy composition, that at least for the observed cellular structure, solidification is due to the growth in a positive temperature gradient. On the other hand, it was interpreted [5] the similarity of the microstructures in melt spun and bulk undercooled Cu-Ni-alloys as an experimental verification of the growth of the solid/liquid interface in an undercooled melt. Using a piston and anvil splat cooling technique, it was reported [6] temperature measurements during the cooling procedure which show high initial undercooling of the melt prior to solidification. Furthermore, the abrupt transition from a well-known needle-like structure in bulk undercooled samples to an equiaxed fine-grain structure [7–13] following pronounced initial bulk undercooling is discussed in the literature as either a steep increase in the nucleation rate in the melt or, alternately, a post-solidification transformation.

In the present paper the results of a comparative study of the microstructure of bulk undercooled and melt spun ribbons are reported in analogy to the abovecited. Fe-Si- and Ni-Si-alloys were selected because of the different crystal structure of the solid solutions and the technical importance of Fe-Si-ribbons.

2. Experimental procedure

The master alloys were prepared from hydrogen-purified iron (99.99%), electrolytic nickel (99.99%) and semiconductor grade silicon by radio-frequency induction melting in alumina crucibles under an inert atmosphere. The same arrangement was used to undercool samples of about 40 g under a Mo-glass slag. Further details are given in [14]. The temperature of the melt was followed by thermocouples with a relative accuracy of ± 10 K. The average composition of the master alloys and of the rapidly quenched ribbons was controled by X-ray fluorescence analysis. The planar flow casting (PFC) process using quartz nozzles with rectangular slits ($0.6 \times 12 \div 0.8 \times 12$ mm^2 at a distance of 100–400 μm over the wheel was used for ribbon preparation in air (copper and steel wheel) or under an atmosphere of CO_2 (steel wheel) for a reduction

of lift-off. Furthermore, ribbons were produced by a double roller technique (DRT) [15] equipped with steel wheels and operating in air. The nominal silicon content of the iron based ribbons was 6.5 wt%Si. Circumferential speed of the wheel(s) were varied between 3 and 30 m/s (PFC) and 1 and 12 m/s (DRT), resp.. The macro- and microstructures of different cuts of the ingots or the ribbons were studied by optical metallography after a mechanical grinding and polishing procedure and etching in 5 mol alcoholic HNO_3. The level of microstresses of the solidified specimen was characterized by X-ray profile analysis using the $\{200\}_\alpha$- and $\{400\}_\alpha$-reflexes and Ni-K_α-radiation for Ni-alloys and $\{110\}_\alpha$- and $\{220\}_\alpha$-reflexes and Fe-K_α-radiation for Fe-alloys, respectively.

3. Results and discussion

3.1. Bulk undercooled melts

At low and medium undercooling ΔT, solidification of Fe-Si and Ni-Si-alloys is characterized by an usually dendritic structure with decreasing characteristic dimensions with increasing ΔT. Crystallization of the whole undercooled volume is initiated by a single nucleus if supercooling is higher than about 50–60 K. This is concluded from the radial distribution of the dendrites emanating from a single nucleation centre (Fig. la). For $\Delta T_c^* > 190$ K a transition from the dendritic to a simpler cylindrical, needle-like growth morphology without secondary branching is observed for Fe-5 wt%Si and Ni-3.7wt%Si-alloys (Fig. lb). Above a second alloy-dependent critical supercooling ΔT_c an abrupt transition from needle-like to a fine equiaxed poligonal grain structure occurs in resolidified pure nickel and Ni-Si-samples. Twins similar to annealing twins in fcc metals are observed (Fig. lc). A corresponding transition at $\Delta T > \Delta T_c$ was reported in [5, 7–13, 20] for pure Ni, Ag, Pd and Cu and their single-phase binary alloys (fcc structure). But in contrast to [7–9] the observed abrupt transition to a spherical microstructure at $\Delta T > \Delta T_c$ for Ni and its alloys is not explained by a pressure-enhanced nucleation but by secondary processes, especially by primary recrystallization during the cooling procedure after recalescence. At the same time we assume that significant contribution in transformation of primary structure can be introduced by processes of dendrite structure coarsening by mechanism of dendrite trunks fragmentation, remelting and secondary branches coalescence as well. These processes have been considered in [21–24] both theoretically and experimentally. However we did not observe such processes in Fe-5wt%Si-samples supercooled up to the maximum attainable $\Delta T \approx 300$ K. (cooling rate 10 K/s). Again, the lateral dimensions of the needle-like structure decreased with increasing bath undercooling (Fig. 2). These general features of structure evolution as a function of bath undercooling agree well with the literature [5].

The recrystallization mechanism of structure refinement in Ni and its alloys is confirmed by the concentration dependence of ΔT_c given in Fig. 3. ΔT_c increases from 145 K for pure Ni to 225 K for Ni-3.7wt%Si because of the wellknown influence of solutes to

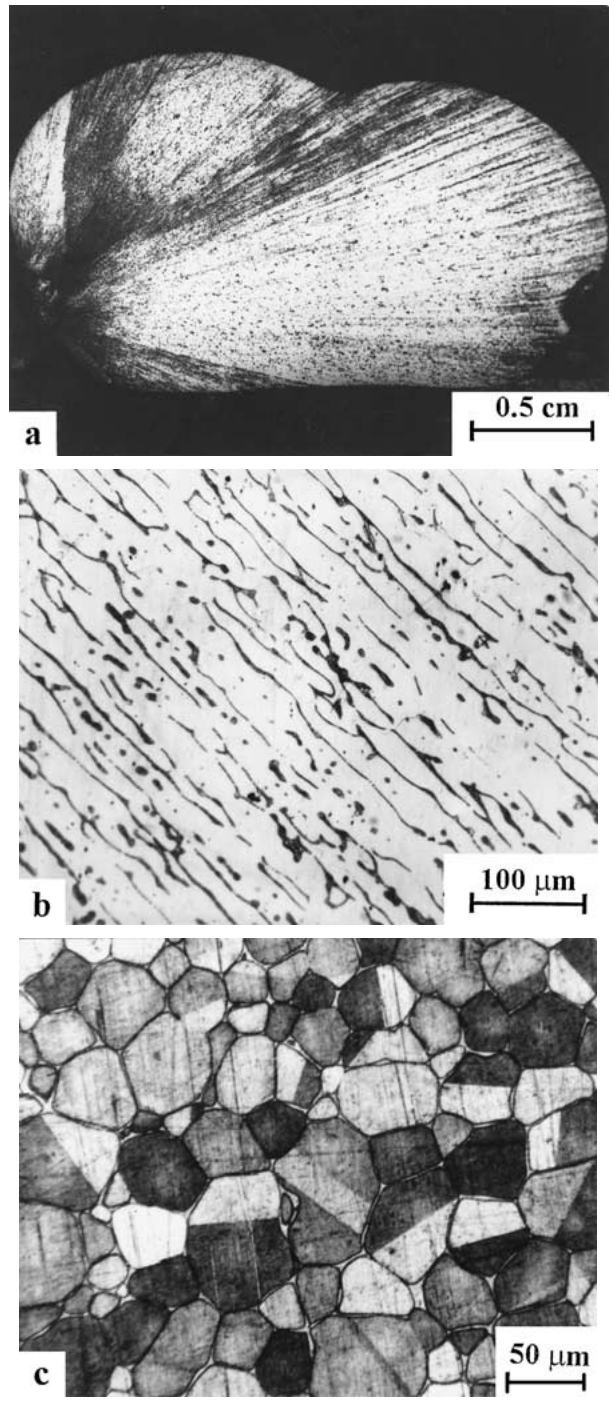

Figure 1 Microstructure of bulk undercooled samples, 1a, b: Fe-5wt.%Si; $\Delta T = 270$ K, lc: Ni-3.7wt.% Si, $\Delta T = 240$ K.

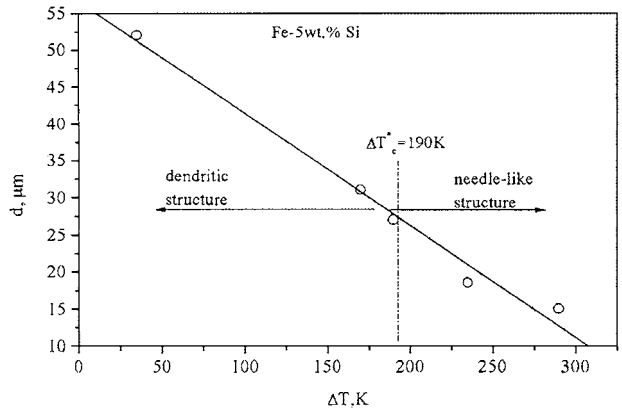

Figure 2 Average linear dimension of the needle-like structure (d) as a function of bath undercooling (ΔT) in Fe-5wt%Si-samples.

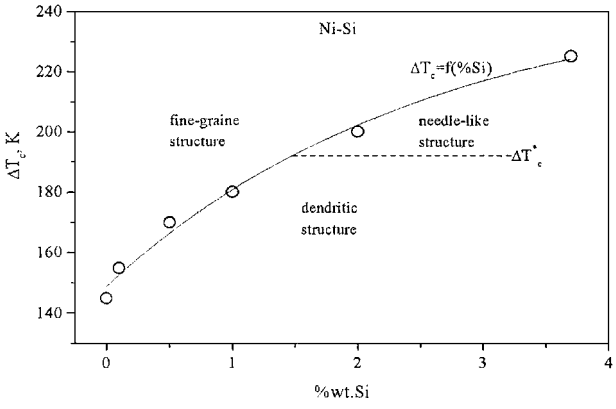

Figure 3 The dependence of the critical bath undercooling (ΔT_c) on the Si-content in Ni-Si-alloys [16].

reduce recrystallization kinetics. Therefore, region of supercoolings characterized by preservation of primary structure is extended in Ni-alloys. This is the reason why in Ni-(2.0–3.7)wt%Si at $\Delta T > 190$ K the needle-like structure was formed whereas in pure Ni and Ni < 2.0wt%Si-alloys branched dendrites are observed up to ΔT_c, only. Since recrystalization in bcc alloys in contrast to fcc alloys ones is hindered, needle-like structure, which forms in Fe-5%Si at 190 K, remains up to maximum $\Delta T = 300$ K and no structure refinement occurs. The same behaviour was found for single-phase Fe-Sn, Fe-Mo and Fe-W-alloys [25].

Described above transition from dendritic structure to needle-like (spherulitic) one was observed for the first time during investigation of morphology and kinetics of cyclohexanol crystals growing from supercooled melt [26, 27]. Crystal rounding occured for this is treated in the theory [28] as transition to steady-state growth at $\Delta T_{hyp} = \Delta H_f / C_p$ (ΔH_f—enthalpy of crystallization, C_p—specific heat capacity), or at achievement of maximum growth rate V_{max} on the dependence $V(\Delta T)$ [29]. Investigations carried out by us in [30] on succinonitrile model alloys with 10, 15, 30, and 48 wt% of salol have shown that independently from salol concentration at the same $\Delta T_c^* = 15$ K transition occurs also to macroscopically rounded spherulitic growth form though both $\Delta T_{hyp} = 45$ K and V_{max} don't be achieved for this. These results in totality with obtained ones on metallic alloys [14, 16–22, 25] give evidence that degeneration of dendritic growth form and formation of needle-like (spherulitic) structure at ΔT_c^* is general rule of solidification of typical metals and other low-entropy substances under highly nonequilibrium conditions. It should be noted also that kinetics of succinonitrile crystal growth in the whole investigated temperature region (up to $\Delta T = 20$ K) is described by dependence $V = K(\Delta T)^n$ where n decreases appropriately from 2,4 (succinonitrile) to 1,5 (48 wt% of salol) reflecting hindering effect of the second component on crystal growth. This contradicts to data [31–33] according to which character of dependence $V(\Delta T)$ for metals and alloys investigated in these works changes from exponential with $n = 3$ to linear at $\Delta T = 170$–190 K. This is possibly connected with fact that fast-acting registration apparatus used in these works gives only average information about shift of the whole crystallization front but not tip of dendrite or needle.

3.2. Rapidly quenched ribbons

Fig. 4a and b show optical micrographs of longitudinal sections of ribbons spun by PFC and DRT on steel wheels, respectively. Fig. 4c gives a schematic representation of the thickness dependence of the microstructure for PFC-ribbons. In full agreement with other investigators [34–36] two types of grain structure were found:

- a very thin (1–3 μm) layer parallel to the wheel surface with an equiaxed structure,
- columnar grains emanating from the equiaxed chill region and growing normal for some distance from the wheel before bending toward the direction of ribbon formation (PFC) or without any preferential orientation (DRT).

Inside the columnar grains a well pronounced needle-like structure is observed reaching up to the free surface of the ribbons (Fig. 5) which is very similar to that of Fe-Si-samples solidified after bulk undercooling with $\Delta T < \Delta T_c^*$. The needlelike structure exhibited the same curved behaviour in the columnar grains in PFC. In DRT-ribbons the needles did not show this bending at all. The equiaxed chill layer is free from dendrites. Compared with Fig. 2, the characteristic linear dimensions of the needle-like structure of the ribbons measured perpendicular to the needle axis is significantly lower. Its dependence on the ribbon thickness (PFC) and the half thickness of ribbons (DRT), resp., is given in Fig. 6 for Fe-6.5 wt%Si. Using the $d(\Delta T)$-dependence in Fig. 2 and the measured range for the ribbons (0.7–1.5 μm) a bath undercooling of the melt in rapid quenching around $\Delta T \approx 400$ K is estimated.

The average grain size $\bar{D}_1$ (see Fig. 4c for definition) as a function of the ribbon thickness (PFC) or the half thickness (DRT), resp., is shown in Fig. 7. Some results taken from the literature are included for comparison. As can be seen, $\bar{D}_1$ seems to increase approximately linearly up to $h = 30\,\mu$m for PFC-ribbons. Then, inside the columnar grains with needle-like substructure smaller polygonal grains became visible which probably exibit a higher density near the wheel surface of the ribbon. The average diameter $\bar{D}_2$ (see Fig. 4b) of these "secondary" grains increases with increasing thickness of the ribbon. At the same time the needle-like structure disappears due to homogeneization of the microsegregation connected with the dendritic growth morphology. It follows that for $h > 30\,\mu$m the observed microstructure is the result of the solidification process as well as of post-solidification transformation. The above-described formation of a secondary grain structure in as-quenched ribbons of Fe-6.5wt%Si is very similar to the structure refinement observed in supercooled pure and Si-alloyed Ni at $\Delta T > \Delta T_c$.

At this point the driving forces for the autonomous solid state transformation process must be discussed. Obviously, rapid solidification will result in a higher density of dislocations, excess vacancies [37], and internal stresses caused by inhomogeneous solute distribution and complex temperature fields during the cooling compared with equilibrium solidification. With a further increase of bath supercooling ΔT these internal

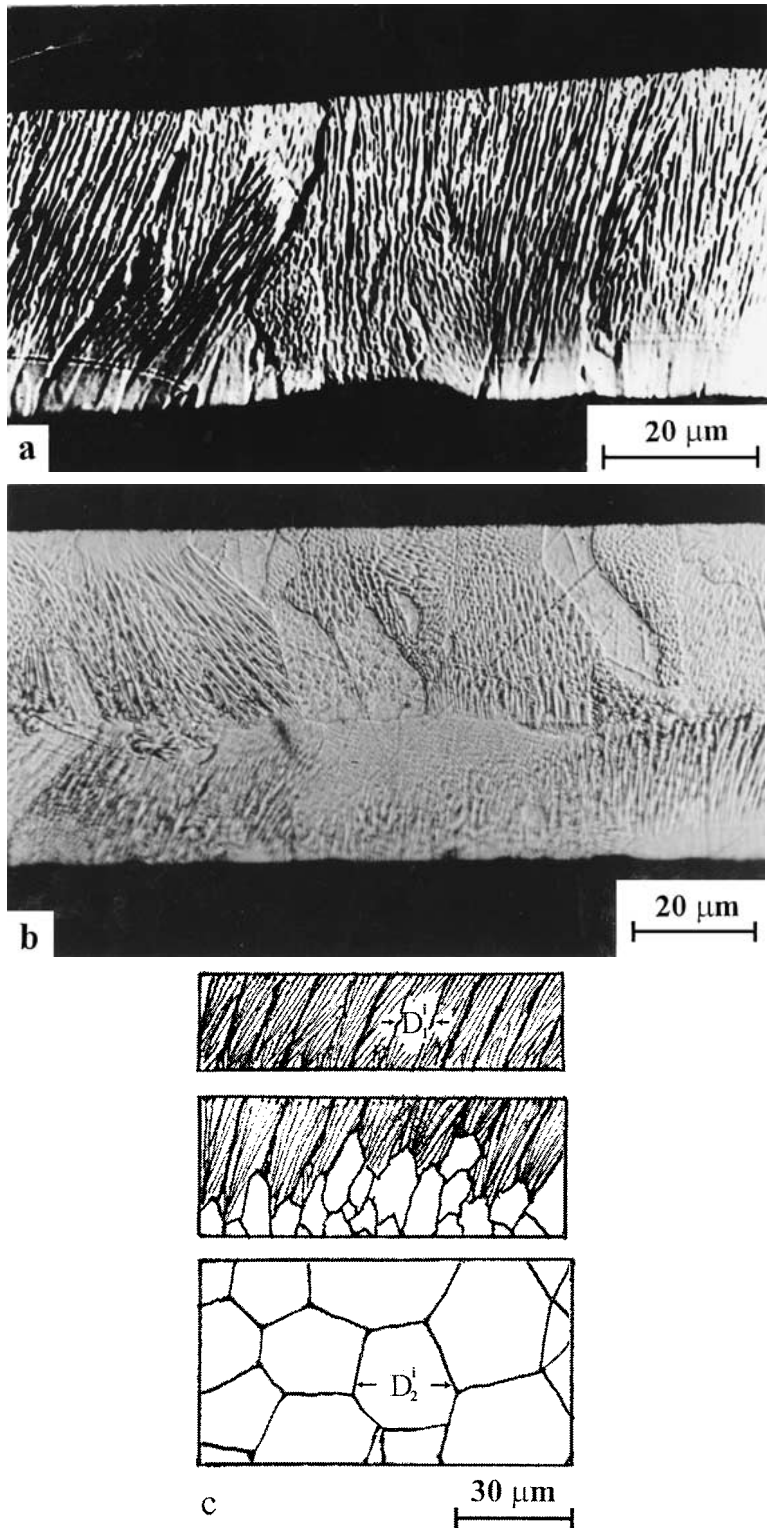

Figure 4 Micrographs of longitudinal sections of Fe-6.5wt.% Si-ribbons prepared by PFC (a) and DRT (b), resp., and schematically for PFC (c).

stresses can reach a critical value and cause recrystallization during the cooling procedure.

Indeed, in a previous paper [18] it was shown that in Ni-3.7wt%Si the second-order internal stresses characterized by $\Delta a/a$ increase with increasing supercooling (Fig. 8) up to $\Delta T \approx 225$ K, followed by an abrupt decrease to stress levels typical for well-annealed material. At the same time the transition from needle-like to spherical structure took place. A further increase of the bath supercooling did not alter the stress level in the resolidified samples. In contract to this behaviour, but in agreement with the above-mentioned microstructural peculiarities (absence of the spherical structure), $\Delta a/a$ for supercooled Fe-5wt%Si monotonically increased with increasing bath supercooling (Fig. 8). The different initial slope of $\Delta a/a = f(\Delta T)$ for Fe-Si can be attributed to a stress reduction due to dynamical recovery (polygonization) preceding recrystallization, which is often observed in bcc alloys. Subgrain boundaries arranged approximately perpendicular to the needles can be regarded as an experimental verification of a rearrangement of dislocations.

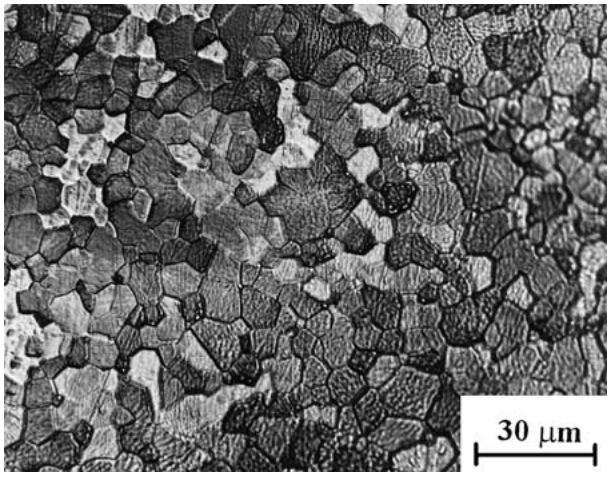

Figure 5 Micrograph of the free surface of a Fe-6.5wt.% Si-PFC-ribbon ($h = 35\ \mu$m).

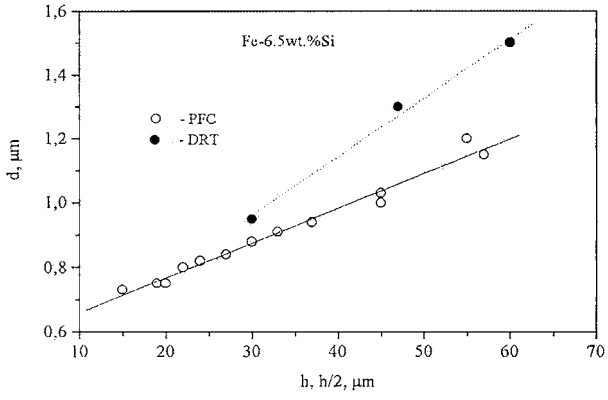

Figure 6 Average linear dimension of the needle-like structure (d) as a function of the thickness of the ribbons.

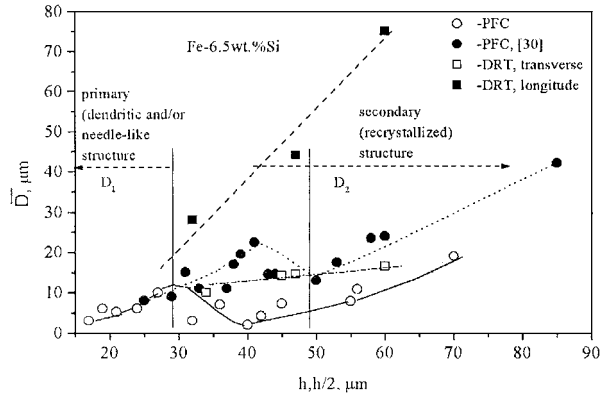

Figure 7 Average grain size perpendicular to the normal of the ribbon (D) as a function of the thickness (partly taken from [34]).

In Fig. 9 $\Delta a/a$ is shown as a function of the ribbon thickness for PFC using two different wheel materials. The maximum lattice distortion is correlated with the thinnest ribbon which can be described by the largest bath undercooling (see Fig. 4). $\Delta a/a$ decreases steeply with increasing thickness of the ribbons. The maximum $\Delta a/a$ for ribbons is significantly higher compared with bulk supercooled samples, in agreement with the predicted higher supercooling. Comparing Figs 7 and 9 one can conclude that the level of internal stresses attainable by rapid quenching and the thickness dependent cooling characteristics allow for a recrystallization of the primary grain structure (grain refinement) if the

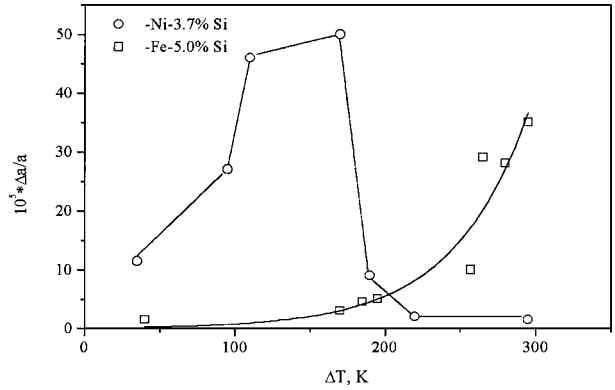

Figure 8 Dependence of internal stresses characterized by $\Delta a/a$ as a function of bulk undercolling for Fe-5wt.%Si and Ni-3.7wt.%Si-alloys.

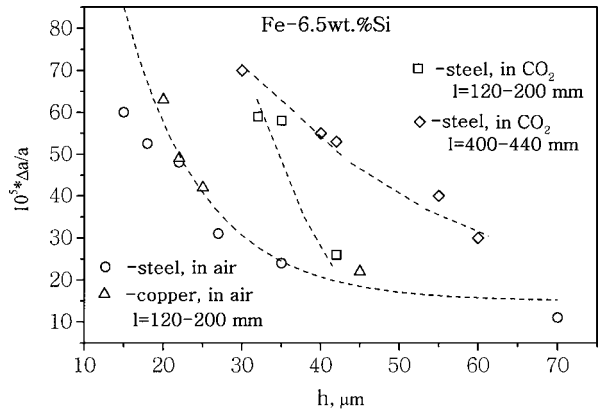

Figure 9 $\Delta a/a$ as a function of the ribbon thickness (h) for Fe-6.5wt.%Si-ribbons.

thickness of the ribbons is in the range $h = 30$–$40\ \mu$m. In spite of the high level of internal stresses for thinner ribbons, the ribbon residence time at temperatures sufficient for noticeable recrystallization is too small. Connected with this the ribbon usually exibits a well pronounced curvature parallel and perpendicular to the axis of the ribbon. The superposition of primary and secondary structures, the degree of which surely depends on the actual conditions of ribbon formation, will result in a very complex inhomogeneous grain structure. If this grain structure is to be described by an average grain size $\bar{D}$ one must keep in mind that it is given by $\bar{D} = (\Sigma D_1^i + \Sigma D_2^i)/(n_1 + n_2)$, where n_1 and n_2 are the numbers of primary and secondary grains and D_1^i and D_2^i their dimensions, resp. At a small thickness of the ribbon ($h < 30\ \mu$m), $n_2 = 0$ is valid because of the absence of recrystallization, and the average grain size is then determined by the primary grain size only. In the transition range (30–50 μm), average grain size $\bar{D}$ will decrease because of $D_1^i > D_2^i$, leading to a minimum in the function $\bar{D}(h)$. Then, with a further increase of h, n_1 turns to zero and D_2^i increases, $\bar{D}$ is than determined by the grain size of the recrystallized structure. For h, $h/2 > 70\ \mu$m, the primary structure is fully transformed. With the above-mentioned arguments the dependence of the average grain size on the thickness of the ribbons given in Fig. 7 can be explained.

The attainable ΔT and the cooling characteristics to room temperature determining the resulting microstructure of ribbons depend on many technological and technical parameters like superheating of the melt,

wetting behaviour, heat transfer coefficient, length of ribbon/wheel contact. Preparing, for example, a PFC-Fe-6.5wt%Si-ribbon under an atmosphere of CO_2, the lift-off could be almost totally avoided. This leads to a microstructure characterized by a smaller average grain size and needle diameter which transforms at greater thicknesses as compared with a ribbon with a high density of lift-off.

4. Summary

Microstructural features of rapidly quenched Fe-6.5wt%Si-ribbons prepared both by a planar flow casting and double roller technique were compared with those of resolidified bulk undercooled Ni-Si- and Fe-Si-alloys. The following conclusions can be drawn from this investigation:

- Solidification of melt-spun ribbons is due to growth of the solid in an undercooled melt (similarity of microstructures).
- The bath undercooling prior to solidification of the ribbons is greater than the maximum undercooling attainable in bulk undercooling experiments (smaller linear dimensions of the comparable needle-like structures).
- Solidification at rapid quenching is connected with the formation of internal stresses, which can lead to secondary reactions in the solid like recrystallization during recalescence and cooling down to room temperature (existence of a critical bulk undercooling for the transition to spherical microstructures).
- The extent of secondary reactions depends on the post-solidification cooling procedure and leads to a thickness dependence of the microstructure of the ribbons.
- Formation of needle-like (spherulitic) structure is law of solidification under highly non-equilibrium conditions independently from method of their realization and don't connected with transition to steady-state growth.

Acknowledgement

The authors would like to express their appreciation to Pr. D. E. Ovsienko and Dr. R. Sellger for many valuable discussions and the critical reading of the paper.

References

1. R. SELLGER, W. LOSER and W. NEUMANN, *J. Mater. Sci.* **19** (1984) 2145.
2. H. JONES, *Mater. Sci. Eng.* **65** (1984) 145.
3. L. J. MASUR and M. C. FLEMINGS, in "Rapidly Quenched Metals, RQ 4," edited by T. T. Masumoto and K. Suzuki (The Japan Institute of Metals, Sendai, Japan, 1982) p. 1557.
4. S. N. TEWARI and T. K. GLASGOW, *Met. Transactions* **18A** (1987) 1663.
5. C. CAESAR, U. KOSTER, R. WILLNECKER and D. M. HERLACH, *Mater. Sci. Eng.* **98** (1988) 339.
6. I. S. MIROSHNICHENKO, "Zakalka iz zidkogo sostojania" (Metallurgija, Moskva, 1982) in Russian.
7. J. L. WALKER, in "Physical Chemistry of Process Metallurgy," edited by G. R. St. Pierr (AIME, New York, 1961) p. 845.
8. G. A. COLLIGAN, V. SURPRENANNT and F. LEMKEY, *J. Metals* **13** (1961) 691.
9. G. FEHLING and E. SCHEIL, *Z. Metallkunde* **53** (1962) 593.
10. B. L. JONES and G. M. WESTEN, *J. Mater. Sci.* **5** (1970) 843.
11. G. L. F. POWELL, *Trans. AIME* **245** (1969) 1969.
12. G. L. F. POWELL and L. M. HOGAN, *ibid.* **245** (1969) 407.
13. L. A. TARSHIS, J. L. WALKER and G. W. RUTTER, *Met. Trans.* **9** (1971) 2589.
14. D. E. OVSIENKO, V. P. KOSTUSHENKO, V. V. MASLOV and G. A. ALFINTSEV, in "Mekhanism i kinetika kristallisazii" (Nauka i Technika, Minsk, 1973) p. 75 (in Russian).
15. J. BRANZOVSKY, M. JURISCH, V. V. MASLOV, V. K. NOSENKO *et al.*, *Mat. Science Eng.* **98** (1988) 75.
16. D. E. OVSIENKO, V. V. MASLOV, G. A. ALFINTSEV *et al.*, *Isvest. Akad. Nauk USSR, Metalli* **5** (1976) 114 (in Russian).
17. G. A. ALFINTSEV, D. E. OVSIENKO, N. V. STOICHEV and V. V. MASLOV, in "Mekhanism i Kinetika Kristallisazii" (Nauka i Technika, Minsk, 1973) p. 332 (in Russian).
18. D. E. OVSIENKO, V. V. MASLOV and V. N. DNEPRENKO, *Izvest. Akad. Nauk, Metalli* **9** (1979) 138 (in Russian).
19. D. E. OVSIENKO, G. A. ALFINTSEV and V. V. MASLOV, *J. Cryst. Growth* **26** (1974) 233.
20. E. SCHLEIP, R. WILLNECKER, D. M. HERLACH and G. P. GORLER, *Mater. Sci Eng.* **98** (1988) 39.
21. M. C. FLEMINGS, "Solidification Processing" (McGraw-Hill, New York, 1974).
22. D. M. HERLACH, *Mater. Sci Eng.* A **226–228** (1997) 348.
23. M. SCHWARZ, A. KARMA, K. ECKLER and D. M. HERLACH, *Phys. Rew. Lett.* **73** (1994) 1380.
24. A. KARMA, *Int. J. Non-Equil. Proc.* **11** (1998) 201.
25. D. E. OVSIENKO, V. V. MASLOV and G. A. ALFINTSEV, in "Problemi stalnogo slitka" (Mettallurgia, Moskva, 1975) in Russian.
26. D. E. OVSIENKO, G. A. ALFINTSEV and A. V. MOHORT, in "Rost cristallov" (Nauka, Moskva, 1972) 162 (in Russian).
27. D. E. OVSIENKO and G. A. ALFINTSEV, in "Crystals Growth, Properties and Applications," edited by H. C. Freyhardt (Springer-Verlag, Berlin, 1980) p. 120.
28. A. P. UMANTSEV, V. V. VINOGRADOV and V. T. BORISOV, *Crystallographija* **31** (1986) 1002 (in Russian).
29. D. E. TEMKIN and V. B. POLIAKOV, *ibid* **21** (1976) 661 (in Russian).
30. A. G. BORISOV, O. P. FEDOROV and V. V. MASLOV, *ibid.* **36** (1991) 1267 (in Russian).
31. R. WILLNECKER, D. M. HERLACH and B. FENERBACHER, *Appl. Phys. Lett.* **56** (1990) 324.
32. K. ECKLER, R. F. COCHRAN, D. M. HERLACH and B. FENERBACHER, *Mat, Sci. and Eng.* A **133** (1991) 702.
33. R. F. COCHRAN, A. L. GREER, K. ECKLER and D. M. HERLACH, A **133** (1991) 698.
34. E. VOGT and G. FROMMEYER, in "Rapidly Solidified Mater," edited by P. E. Lee and R. S. Carbonara, (ASM, 1986) p. 291.
35. K. I. ARAI, H. TSUTSUMITAKE and K. OHMORI, *Trans. Jap. Inst. Metals* **25** (1984) 855.
36. F. KOGITZU, M. YUKAMOTO, K. SHIBUYA *et al.*, in "Rapidly Solidified Alloys and Their Mech. and Mag. Properties," edited by B. C. Giessen, E. Polk and A. I. Taub (Met. Res. Symp. Proc., 1986) p. 15.
37. A. M. GLEZER, B. V. MOLOTILOV and V. V. SOSNIN, *Isvest. Akad. Nauk SSSR, Fizika* **49** 1985 1602 (in Russian).

Received 20 September 2001
and accepted 25 July 2002